Competition of superconductivity with the structural transition in Mo_3Sb_7

G. Z. Ye,[1,2] J.-G. Cheng,[1,3,*] J.-Q. Yan,[4] J. P. Sun,[1] K. Matsubayashi,[3,5] T. Yamauchi,[3] T. Okada,[3] Q. Zhou,[2] D. S. Parker,[4] B. C. Sales,[4] and Y. Uwatoko[3]

[1]*Beijing National Laboratory for Condensed Matter Physics and Institute of Physics, Chinese Academy of Sciences, Beijing 100190, China*

[2]*School of Physical Science and Astronomy, Yunnan University, Kunming 650091, China*

[3]*Institute for Solid State Physics, University of Tokyo, Kashiwa, Chiba 277-8581, Japan*

[4]*Materials Science and Technology Division, Oak Ridge National Laboratory, Oak Ridge, Tennessee 37831, USA*

[5]*Department of Engineering Science, University of Electro-Communications, Chofu, Tokyo 182-8585, Japan*

(Received 20 September 2016; revised manuscript received 9 November 2016; published 14 December 2016)

Prior to the superconducting transition at $T_c \approx 2.3$ K, Mo_3Sb_7 undergoes a symmetry-lowering, cubic-to-tetragonal structural transition at $T_s = 53$ K. We have monitored the pressure dependence of these two transitions by measuring the resistivity of Mo_3Sb_7 single crystals under various hydrostatic pressures up to 15 GPa. The application of external pressure enhances T_c but suppresses T_s until $P_c \approx 10$ GPa, above which a pressure-induced first-order structural transition takes place and is manifested by the phase coexistence in the pressure range $8 \leqslant P \leqslant 12$ GPa. The cubic phase above 12 GPa is also found to be superconducting with a higher $T_c \approx 6$ K that decreases slightly with further increasing pressure. The variations with pressure of T_c and T_s satisfy the Bilbro-McMillan equation, i.e. $T_c^{\,n} T_s^{\,1-n} =$ constant, thus suggesting the competition of superconductivity with the structural transition that has been proposed to be accompanied with a spin-gap formation at T_s. Our first-principles calculations suggest the importance of magnetism that competes with the superconductivity in Mo_3Sb_7.

DOI: 10.1103/PhysRevB.94.224508

I. INTRODUCTION

In recent years, quantum criticality has been considered as a universal organizing principle for several families of unconventional superconductors [1], including the heavy-Fermion, cuprate, and iron-based high-T_c superconductors, in which the superconducting transition temperature T_c can usually be enhanced by suppressing a competing electronic order in the normal state via chemical doping or the application of high pressure. To unravel the competitive nature of superconductivity with other electronic orders can not only clarify the key factors governing T_c, but also deepen our understanding on the pairing mechanism for the observed superconductivity. In this paper, we have applied this approach to reveal a competitive coexistence of superconductivity with a structural transition in Mo_3Sb_7 that has been suggested to be a model system to study the interplay between superconductivity, magnetism, and structural transition [2,3].

Mo_3Sb_7 has been known since the 1960s as the only compound in the Mo-Sb binary system [4]. The revival of interest in this compound arises from the recent discovery of superconductivity below $T_c \approx 2.1$ K as well as the promising thermoelectric properties upon proper doping [5–7]. Although much effort has been devoted to clarify the pairing mechanism of superconductivity, there has been no consensus reached so far. Point-contact Andreev-reflection measurements found a strong anisotropy of the superconducting gap parameter $\Delta(\Delta_{max}/\Delta_{min} > 40)$, suggesting an unconventional $(s+g)$-wave pairing symmetry [8,9]. In contrast, specific-heat, nuclear quadrupole resonance, and muon-spin-ration studies on Mo_3Sb_7 support a conventional s-wave Bardeen-Cooper-Schrieffer (BCS) superconductor; however, it remains under debate whether the superconducting state consists of a single, isotropic gap or two different gaps [10–15]. Moreover, Mo_3Sb_7 has been suggested as a coexistent superconductor-spin fluctuation system, in which the observed T_c can be explained only after considering the paramagnon effect in the McMillan equation [16]. Tran *et al.* [17] studied the electrical and magnetic properties of polycrystalline Mo_3Sb_7 under pressures up to 2.2 GPa in the temperature range 0.4–80 K. They proposed a pressure-induced spin density wave competes with superconductivity. These arguments point to an unconventional nature of the observed superconductivity and might have a deep root in the peculiar normal state.

Mo_3Sb_7 crystallizes in the Ir_3Ge_7-type cubic structure with space group Im-$3m$ at room temperature [18]. The Mo sublattice is characterized by a three-dimensional network of Mo-Mo dumbbells formed by the nearest-neighbor (NN) bond of ~3 Å. Alternatively, the Mo sublattice can be regarded as Mo6 octahedral cages at the body-centered positions; these octahedral cages are formed by the next-NN (NNN) Mo-Mo bond of ~4.6 Å and are connected with each other by the NN bond, as shown in Fig. 1(a). Prior to the superconductivity transition, Mo_3Sb_7 undergoes a symmetry-lowering, cubic-to-tetragonal structural transition at $T_s \approx 53$ K. Previous studies have suggested that the structural transition at T_s is accompanied with the opening of a spin pseudogap of $\Delta_s/\kappa_B \approx 120$ K, which has been attributed to the formation of Mo-Mo spin-singlet dimers [15,19–21]. The importance of magnetism on the structural transition has also been highlighted in a recent study on the lightly doped Mo_3Sb_7 [3]. The fact that the NN Mo-Mo bond length along the c axis is about 0.3% shorter than those within the ab plane in the tetragonal phase, Fig. 1(b), indicated that the spin-singlet states could occur only along the c axis, leaving the remaining conduction 4d electrons of Mo forming the superconductivity states below T_c [22]. Such a scenario could make Mo_3Sb_7 a

*jgcheng@iphy.ac.cn

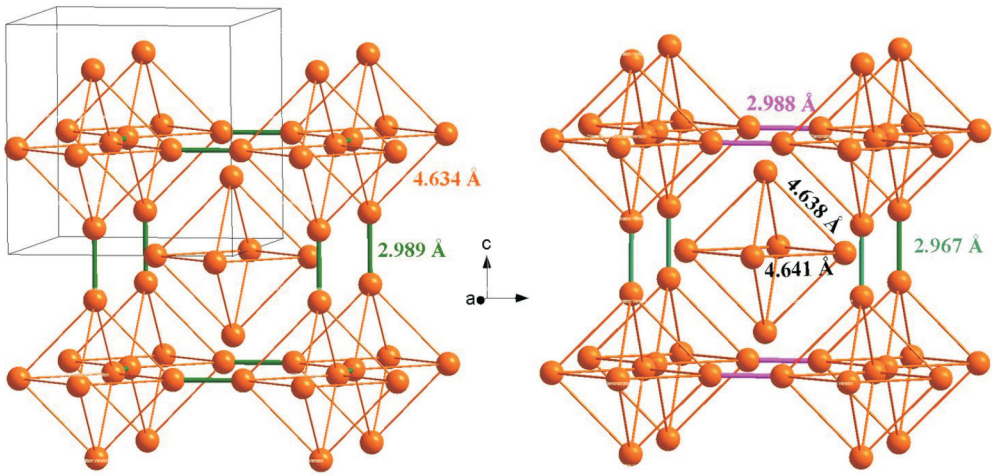

FIG. 1. The Mo sublattice of Mo_3Sb_7 that consists of Mo6 octahedral cages at the body-center positions formed by the NNN Mo-Mo bond of ~4.6 Å and connected via the NN Mo-Mo bond of ~3 Å in the cubic (left) and tetragonal (right) phase. The NN Mo-Mo bond length along the c axis is about 0.3% shorter than those within the ab plane in the tetragonal phase [21].

rare example where the localized spin-singlet states coexist with superconducting states below T_c [22]. This might be responsible for the above-mentioned contradictions about the mechanism of superconductivity. Although the issue of whether there is any correlation between T_s and T_c has been raised before [19], direct evidence to confirm the competitive nature of superconductivity with the structural transition or the spin-singlet states remains lacking. In addition, with a structural transition and spin-gap formation above the superconductivity transition, Mo_3Sb_7 can be also regarded as an interesting system to explore the quantum criticality with an intimated interplay between lattice instability, magnetism, and superconductivity [2,3]. By utilizing high pressure as a clean tuning knob, we demonstrate in this paper the competitive coexistence of superconductivity with the structural transition, which should serve as a constraint when discussing the mechanism of observed superconductivity in Mo_3Sb_7.

II. EXPERIMENTAL DETAILS

Single crystals of Mo_3Sb_7 used in this paper were grown out of Sb flux. Detailed characterizations on the structural transition and physical properties at the normal and superconducting states have been given elsewhere [2]. All high-pressure resistivity measurements were performed with the standard four-probe method in two different cubic-anvil-type apparatuses [23,24]. The first one employs a 250-ton hydraulic press to maintain a constant loading force over massive BeCu guide blocks during cooling down to the lowest temperature ~2 K [23], while the second one is a miniature, clamp-type "Palm" cubic-anvil cell [24], which enables integration with a ^{3}He refrigerator. For both cases, the applied uniaxial loading force is converted by a pair of guide blocks to three-axis compression on a cubic solid gasket made of either pyrophyllite or MgO. The sample was immersed in the liquid pressure-transmitting medium contained in a Teflon capsule that was put in the center of the solid gasket. Four gold wires attached on the sample were introduced out of the Teflon capsule and placed to direct contact with the tungsten-carbide or sintered-diamond anvils. The anvil's top sizes of 4 and 2.5 mm have been chosen to generate pressures up to 8 and 15 GPa, respectively. For the constant-force apparatus, the pressure was calibrated at room temperature by monitoring the characteristic resistance change of Bismuth (Bi) at 2.55 and 7.7 GPa [23]; for the Palm cubic-anvil cell, the pressure after clamping was calibrated at low temperatures by monitoring the superconducting transition temperature of lead (Pb) [25]. Our first-principles calculations were performed using the all-electron plane-wave density functional theory code WIEN2K [26] in an attempt to understand the observed pressure effect and the potential relevance of magnetism.

III. RESULTS AND DISCUSSIONS

In this paper, we have studied three different pieces of Mo_3Sb_7 crystals from the same batch; two pieces were measured with the constant-force apparatus, the third with the Palm cubic-anvil cell. The ambient-pressure resistivity $\rho(T)$ shown in Fig. 2(a) is consistent with the previously reported data [2,19], featured by a quick decrease at T_s before finally dropping to zero resistivity at T_c. To better illustrate these transitions, in the following, we define T_s as the maximum of $d\rho/dT$ and T_c as the middle point between 10 and 90% drop of resistivity. As shown in Fig. 2(a) and Table I, these three samples show similar $T_s \approx 46(1)$ K and nearly identical $T_c \approx 2.4(1)$ K, the latter being among the highest T_c ever reported for Mo_3Sb_7. It should be noted that characteristic anomalies can be observed in magnetic susceptibility, specific heat, and resistivity around T_s [2,19], but T_s defined from the maximum of $d\rho/dT$ is slightly lower than that determined directly from the low-temperature structural study [22]. Nevertheless, it allows us to track down the systematic variation of T_s with pressure. As noted previously, the normal-state $\rho(T)$ of Mo_3Sb_7 is featured by a rather small residual resistivity ratio $RRR \equiv \rho(300)/\rho(5\text{ K}) \leqslant 1.5$. Single crystals used in this paper show slightly higher RRR values between 1.77 and 2.37. In addition, we have also performed fitting to the $\rho(T)$ data between T_c and T_s with a gap function, viz.

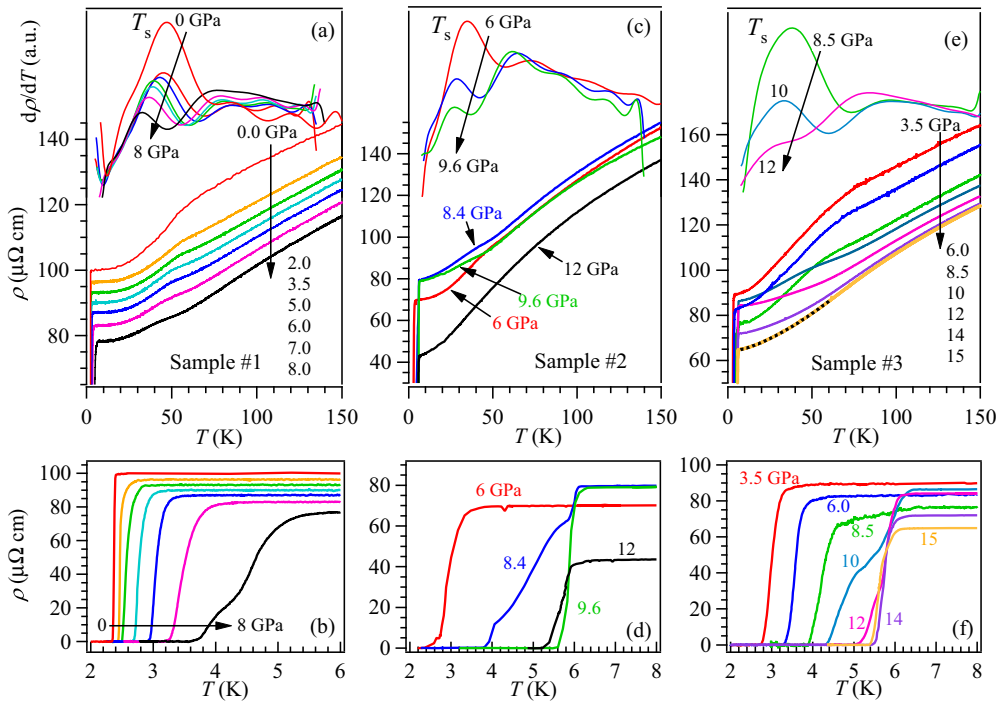

FIG. 2. Temperature dependence of resistivity $\rho(T)$ for (a) and (b) the sample #1 between 2 and 8 GPa, and (c) and (d) the sample #2 between 6 and 12 GPa, both measured with the constant-force cubic-anvil-cell apparatus, and (e) and (f) the sample #3 between 3.5 and 15 GPa measured with the Palm cubic-anvil-cell apparatus. The top panels of (a), (c), and (e) display the temperature derivative $d\rho/dT$ to show the variation of T_s as a function of pressure. (b), (d), and (f) highlight the low-temperature superconducting transition. In (e), the $\rho(T)$ at 15 GPa can be described excellently by $\rho(T) = \rho_0 + AT^\beta$ with $\beta = 1.52(2)$ in a large temperature range $7 < T < 55$ K, shown as the broken curve.

$\rho(T) = \rho_0 + AT + B\exp(-\Delta_s/\kappa_B T)$. The obtained spin gaps of $\Delta_s/\kappa_B \sim 100$ K are also close to the reported values [2,19,20]. The characteristic temperatures and fitting parameters for these three samples are listed in Table I. The above characterizations thus ensure the samples' quality, and we are in the position to present the $\rho(T)$ data under high pressures.

We first loaded the sample #1 in a constant-force apparatus equipped with tungsten-carbide anvils (4 mm top) and measured its resistivity $\rho(T)$ between 2 and 8 GPa. As shown in Fig. 2(a), the $\rho(T)$ in the normal states decreases steadily upon increasing pressure, and the anomaly at T_s shifts down to lower temperatures gradually. In addition, the anomaly at T_s changes from a cusp- to a humplike feature for $P > 5$ GPa. As shown in the top panel of Fig. 2(a), the variation of T_s with pressure can be seen more clearly from the maximum of $d\rho/dT$, whose magnitude also decreases with pressure. In contrast, the superconductivity transition shown in Fig. 2(b) moves up quickly with pressure and reaches about 3.5 K at 7 GPa, where an obvious broad transition is evidenced. Upon further increasing pressure to 8 GPa, the superconducting transition exhibits a two-step feature with the onset temperature over 5 K. The measurements on sample #1 show that the application of external pressure suppresses T_s but enhances T_c. Resistivity measurements under higher pressures are needed to verify: (i) whether the two-step superconducting transition at 8 GPa is caused by an extrinsic pressure inhomogeneity or due to an intrinsic two-phase coexistence, and (ii) how will the T_s evolves with pressure or whether a quantum phase transition can be realized by suppressing completely the cubic-to-tetragonal transition at T_s.

These questions are addressed after measurements on the sample #2 up to 12 GPa by changing the tungsten-carbide anvils to the sintered-diamond anvils. As shown in Figs. 2(c) and 2(d), the following features are noteworthy: (i) the anomaly at T_s decreases continuously and cannot be discerned any more at $P = 12$ GPa; (ii) the two-step superconducting transition is readily observed at $P = 8.4$ GPa, but at 9.6 GPa and above, it changes to a single transition that is coincident with the high-temperature drop of 8.4 GPa data; (iii) T_c decreases slightly with further increasing pressure above 9.6 GPa. These observations unambiguously rule out the extrinsic pressure inhomogeneity as the origin for the two-step superconducting transition, pointing to an intrinsic coexistence of two superconducting phases with different T_c. The

TABLE I. Characteristic temperatures and fitting parameters to the resistivity data for three Mo_3Sb_7 samples measured in this paper.

	Sample No.		
	1	2	3
RRR [$\equiv \rho(300\text{ K})/\rho(5\text{ K})$]	1.77	2.37	1.94
T_c (K)	2.37(2)	2.36(2)	2.35(2)
T_s (K)	46.9	46.6	45.9
$\rho_0(\mu\Omega\,\text{cm})$	99.8(1)	95.0(3)	79.6(3)
$A(10^{-8}\Omega\text{cmK}^{-1})$	4.2(1.2)	11.7(2)	6.9(3)
$B(\mu\Omega\,\text{cm})$	89.5(5)	131.4(9)	6.7.8(5)
Δ_s/κ_B(K)	99(3)	101(5)	83(6)

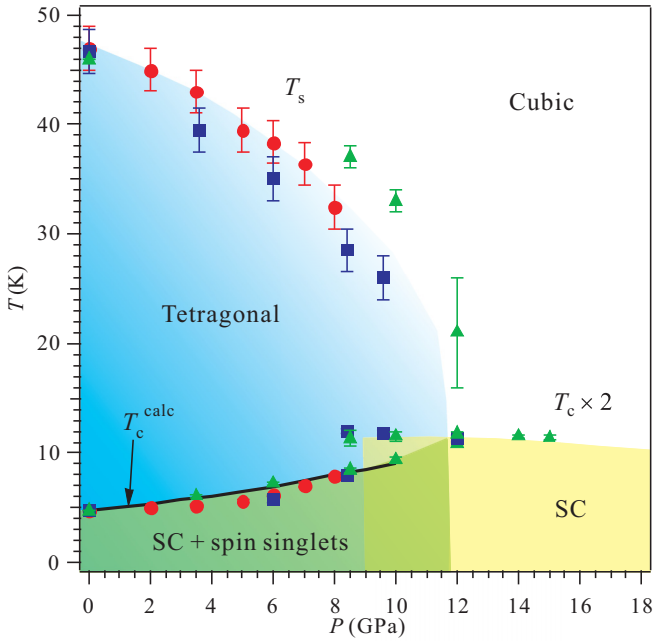

FIG. 3. Temperature-pressure phase diagram of Mo_3Sb_7. The circle, square, and triangle symbols represent the transition temperatures for samples #1, #2, and #3, respectively. The solid black curve denotes the calculated T_c^{calc} according to the Bilbro-McMillan equation, i.e. $T_c^n T_s^{1-n} = T_{c0}$, as detailed in the main text. Note that both the experimental T_c and T_c^{calc} have been scaled by a factor of two.

high-pressure phase above $P_c \approx 10$ GPa should remain cubic down to the lowest temperature and becomes a superconductor with a higher $T_c \approx 6$ K than the low-pressure tetragonal phase. All these observations based on two different samples were further confirmed on the sample #3 measured with a Palm cubic-anvil-cell apparatus up to 15 GPa, as seen in Figs. 2(e) and 2(f). In this case, the two-phase coexistence takes place around 10 GPa, which is about 1.5 GPa higher than that of samples #1 and #2, presumably due to the slight pressure variations upon cooling for the clamp-type Palm cubic-anvil cell. Interestingly, we found that the resistivity at 15 GPa follows excellently the $\rho(T) \sim T^{1.5}$ behavior for $7 < T < 55$ K, signaling the importance of magnetic fluctuations on the incoherent scattering of quasiparticles in the cubic phase above P_c [27,28].

Finally, these results enable us to construct a temperature-pressure (T-P) phase diagram for Mo_3Sb_7 shown in Fig. 3, which depicts explicitly the evolution of the cubic-to-tetragonal structural transition at T_s and the superconducting transition T_c as a function of pressure. It becomes clear that the tetragonal phase is destabilized by pressure, and the cubic phase remains stable down to the lowest temperature at $P \geqslant 12$ GPa. There is a two-phase coexistent region around 10 ± 2 GPa, signaling a first-order character of this pressured-induced phase transition. Within the tetragonal phase at $P < P_c$, the external pressure enhances T_c with a concomitant suppression of T_s, which suggests a competing nature of these two transitions reminiscent of the quantum criticality observed in several unconventional superconductors [1]. The high-pressure cubic phase is also superconducting with higher $T_c \approx 6$ K, which decreases slightly with further increasing pressure. There is a discontinuous jump of T_c from the tetragonal to cubic phases.

Previous studies at ambient pressure have revealed that the cubic-to-tetragonal structural transition at T_s is accompanied with a spin-gap opening [15,19–22], which is most likely associated with the Mo-Mo spin-singlet states formed only along the c axis because the NN Mo-Mo bond is about 0.3% shorter than those within the ab plane in the tetragonal phase, as illustrated in Fig. 1(b). Then the formation of spin-singlet states will produce a gap over part of the Fermi surface (FS) and leave the remaining Mo 4d electrons within the ab plane forming the FS responsible for the observed superconductivity below T_c. By suppressing the spin-singlet states, the application of external pressure restores the missing region of FS and thus increases the density of states (DOS) at Fermi energy available for superconductivity, which could result in the enhancement of T_c. Such a scenario of competition for states at the Fermi energy can be further verified by the Bilbro-McMillan equation [29], viz. $T_c^n T_s^{1-n} = T_{c0}$, where n is the portion of electronic DOS at the Fermi energy forming the superconducting gap, and T_{c0} is the superconducting transition temperature without high-temperature transition at T_s. This relationship was initially developed to account for the competition of superconductivity with the Peierls-like structural transition in A-15 superconductors like V_3Si and Nb_3Sn [29] and was later found to be also applicable in the Chevrel-phase superconductor $Eu_xMo_6S_8$ [30] and the heavy-fermion superconductor $CeRhIn_5$ [31], involving the competition of superconductivity with charge-density-wave and antiferromagnetic transitions, respectively.

To estimate the value of n as a function of pressure, we resorted to the upper critical field $\mu_0 H_{c2}(T)$, whose initial slope $\eta = -\mu_0 d H_{c2}/dT|_{T_c}$ is proportional to the electronic specific-heat coefficient γ and thus $N(E_F)$ via the relationship: $\eta = 4.48\ \gamma\rho_0$ (T/K) in the dirty limit of BCS superconductors [32]. Such a BCS-type relationship has been used successfully to reproduce the experimental value of $\eta = 1.25$ T/K for Mo_3Sb_7 at ambient pressure [12], even though it remains controversial regarding the exact pairing symmetry of superconductivity [6–12]. Figures 4(a)–4(d) show the low-temperature $\rho(T)$ of sample #3 under different magnetic fields and pressures. As can be seen, T_c shifts down to lower temperatures with increasing magnetic fields. Here, we defined T_c as the middle point between 10 and 90% drop of resistivity and plotted the upper critical field $\mu_0 H_{c2}$ as a function of T_c in Fig. 4(e). The initial slope η values are readily obtained from the linear fitting to $\mu_0 H_{c2}(T_c)$, while extrapolations to $T = 0$ allow us to estimate the zero-temperature upper critical fields $\mu_0 H_{c2}(0)$ as 4.0, 5.1, 6.1, 8.9, 8.7, and 8.5 T for $P = 3.5$, 6, 8.5, 12, 14, and 15 GPa, respectively. It is also noteworthy that Mo_3Sb_7 exhibits a relatively large magnetoresistance MR[$\equiv \rho(H)/\rho(0) - 1] > 20\%$ in the normal state just above T_c for $P < P_c$, whereas the MR becomes negligible for $P > P_c$. Further studies are needed to clarify why the relatively large MR is observed in the tetragonal phase.

As shown in Fig. 5, η increases quickly from 1.25 T/K at ambient pressure to 1.52 T/K at 8.5 GPa within the tetragonal phase, which indicates that $N(E_f)$ increases with pressure. On the other hand, η changes slightly in the cubic phase at

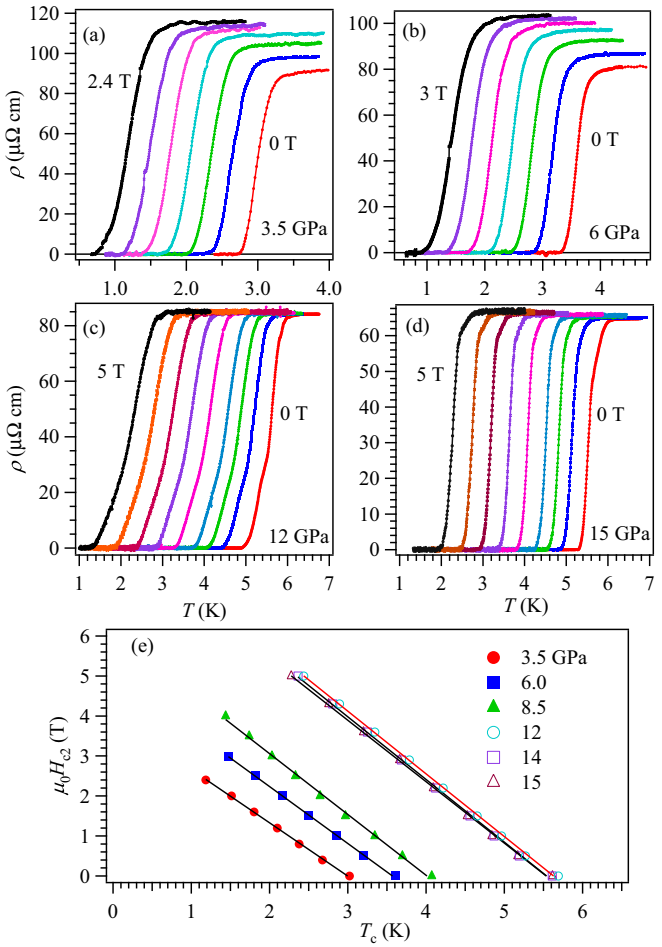

FIG. 4. Magnetic-field dependence of the superconducting transition at different pressures: (a) 3.5 GPa, (b) 6.0 GPa, (c) 12 GPa, and (d) 15 GPa. These data were used to obtain the upper critical fields $\mu_0 H_{c2}$ shown in (e), where a linear fitting has been used to extract the values of initial slope $-dH_{c2}/dT|_{T_c}$.

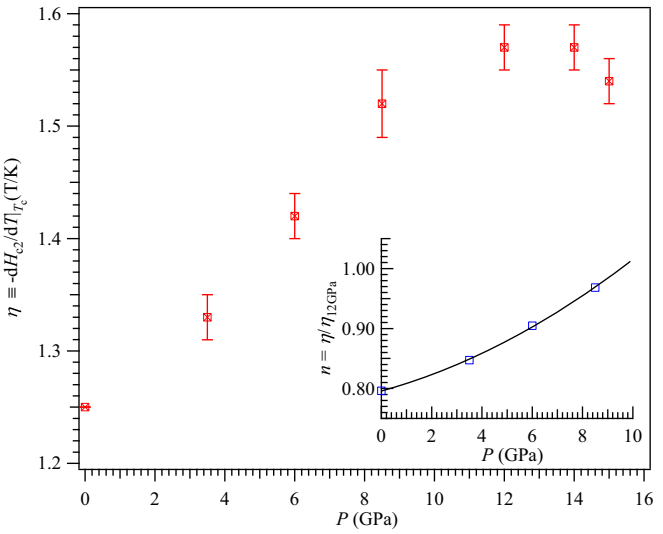

FIG. 5. Pressure dependence of the initial slope of upper critical field $\eta \equiv -dH_{c2}/dT|_{T_c}$. Since η is proportional to electronic specific-heat coefficient γ and thus the DOS at Fermi level $N(E_F)$, we employed the obtained η values below 10 GPa to estimate the portion of electronic states forming the FS $n \equiv \eta/\eta_{12\ \mathrm{GPa}}$ as shown in the inset. Here, we assume all electronic states at 12 GPa participate in the formation of FS since the spin-singlet states vanish at this pressure.

$P >$ 10 GPa. Finally, we obtained $n \equiv \eta/\eta_{12\ \mathrm{GPa}}$ given that the structural transition disappears at 12 GPa. This leads to an $n = 0.8$ at ambient pressure, which indicates that about 20% of the DOS at the Fermi energy is removed below T_s due to the formation of spin-singlet states. From the pressure dependence of n and T_s, we can calculate the pressure dependence of T_c according to the above Bilbro-McMillan equation [29], i.e. $T_c^{\mathrm{calc}} = T_{c0}^{1/n} \cdot T_s^{1-(1/n)}$. As shown by the solid curve in Fig. 3, the experimental T_c can be well reproduced by assuming a $T_{c0} = 4.4$ K, which corresponds to an upper limit of T_c without the high-temperature structural transition. However, this value is lower than the observed $T_c \approx 6$ K for the high-pressure cubic phase. This fact is reflected as a jump rather than a smooth change of T_c near the tetragonal-cubic phase boundary in the T-P phase diagram in Fig. 3, presumably due to the reinforced electron-phonon coupling in the higher symmetry cubic phase as well as the enhanced spin fluctuations as indicated by the non-Fermi-liquid $\rho \sim T^{1.5}$ behavior mentioned above.

We have performed first-principles calculations to further substantiate our experimental findings in this paper. First, our calculations were performed by using the experimental lattice parameters with internal coordinates relaxed until internal forces were less than 2 mRyd/a.u. In this case, the resultant DOS at Fermi level $N(E_F)$ was found to decrease with increasing pressure. This is consistent with the general expectation of pressure decreasing interatomic distances, increasing atomic wave function overlap, thereby causing higher bandwidth and lowering average values of $N(E_F)$. In these calculations, the pressure was introduced by using the experimental lattice parameters.

We found that the $N(E_F)$ values (per Rydberg for both spins) of the tetragonal phase at ambient pressure, 4, and 8 GPa are 281.0, 256.6, 251.9, respectively, and is further reduced to 242.4 at 12 GPa in the cubic phase. This theoretical reduction of $N(E_F)$ with pressure therefore cannot provide an immediate explanation for the experimentally observed enhancement of T_c, which we partially attribute to an increase of $N(E_F)$. To resolve this discrepancy, we have carefully investigated the possible magnetic behavior, which would likely tend to compete with the superconductivity and could also transfer DOS spectral weight away from the Fermi level, thus affecting the observed $N(E_F)$.

In the relaxed structures, we find no evidence of magnetism, with all spin-polarized calculations converging to a result identical to the non-spin-polarized calculations. This is consistent with the lack of magnetism in the tetragonal state, i.e. a temperature-independent magnetic susceptibility below 20 K [2] and the absence of muon spin precession down to 5 K [15]. However, if the experimental internal coordinates are used in the tetragonal state at ambient pressure, we find a ferromagnetic ground state, albeit with small moments (0.025 μ_B per Mo for the fourfold site and 0.073 μ_B per Mo

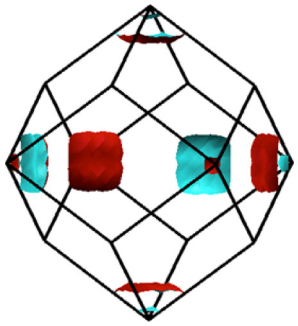

FIG. 6. The calculated FS of band 291 for Mo_3Sb_7 in the tetragonal state [the tetragonal distortion is small so that the Brillouin zone depicted is effectively the body-centered cubic (bcc) zone]. There is a possibility of nesting between the parallel faces.

for the twofold site). A similar situation, i.e. the sensitivity of magnetism to small structural changes, is known in parents of the Fe-based superconductors, as found previously by Subedi *et al.* [33] for the iron chalcogenide FeTe, although in that case, antiferromagnetism was found for the unrelaxed structure.

Here, we find that the nonmagnetic $N(E_F)$ in this unrelaxed tetragonal state 335.6/Ryd-u.c. is some 20% higher than that in the relaxed state, and the Mo-site-projected $N(E_F)$ for the twofold Mo site 35.64/Mo-Ryd is much larger than the relaxed value of 21.53. These large $N(E_F)$ values therefore lead, via the Stoner criterion, to a substantially increased tendency towards ferromagnetism. Calculations initialized in a Mo-Mo nearest neighbor antiferromagnetic configuration also converged to this ferromagnetic state. We now combine this ferromagnetic result with previous theoretical work [34] showing a small magnetic moment configuration to be energetically degenerate with a nonmagnetic state. It is certainly possible, though clearly unproven here, that there is a weak ferromagnetic behavior at ambient pressure. This would tend to compete with the superconductivity, since a spin-singlet superconductivity in general does not coexist with ferromagnetism.

In addition to the possible ferromagnetism inferred from our calculations, there is also the possibility of nesting-based magnetism, which could also compete with the superconductivity. In Fig. 6, we depict the band 291 FS, which from inspection could support a nesting-induced spin-density wave between the parallel faces at the zone corners. Since this FS accounts, from our calculations, for approximately 15% of $N(E_E)$, its gapping [reducing $N(E_F)$] at ambient pressure, and then lack of gapping [thereby increasing $N(E_F)$] as pressure is applied, could yield an increase in the specific heat coefficient with pressure, as we observe experimentally.

These two types of magnetic behavior present possibilities for explaining the observed enhancement of T_c with pressure. It is also possible that there are significant changes in the phonon spectrum, and ultimately electron-phonon coupling λ with pressure, that affect T_c. These would need to be rather significant, given the observed increase in T_c from 2.3 K at ambient pressure to ~6 K at 12 GPa. Using the McMillan [35] equation, this T_c increase would require an approximate 35% increase in λ (from 0.55 to 0.74), assuming a pressure-independent Debye temperature.

IV. CONCLUSION

In summary, we have performed a comprehensive high-pressure study on the resistivity of Mo_3Sb_7 and mapped out the pressure dependence of the cubic-to-tetragonal structural transition and the superconductivity transition up to 15 GPa. Below 10 GPa, pressure suppresses T_s but enhances T_c. A pressure-induced first-order transition takes place in the pressure range 8–12 GPa, above which the cubic phase is stable in the whole temperature range. The high-pressure cubic phase is also a superconductor with higher $T_c \approx 6$ K but shows a negative pressure dependence. Our results demonstrated unambiguously a competitive nature between superconductivity and the structural transition within the tetragonal phase; the lower T_c in the tetragonal phase at ambient pressure arises from the competition with the spin-gap formation. Our first-principles calculations suggest that magnetism should be considered to account for the observed pressure dependence of superconductivity and it may compete with the superconductivity in Mo_3Sb_7. This work further illustrates the close interplay between superconductivity, magnetism, and structural instability in Mo_3Sb_7.

ACKNOWLEDGMENTS

This paper was supported by the National Basic Research Program of China (Grant No. 2014CB921500), the National Science Foundation of China (Grant No. 11574377), the Strategic Priority Research Program and the Key Research Program of Frontier Sciences of the Chinese Academy of Sciences (Grants No. XDB07020100 and No. QYZDB-SSW-SLH013), and the Opening Project of Wuhan National High Magnetic Field Center (Grant No. 2015KF22), Huazhong University of Science and Technology. Work at Oak Ridge National Laboratory was supported by the US Department of Energy, Office of Science, Basic Energy Sciences, Materials Science and Engineering Division.

[1] M. R. Norman, Science **332**, 196 (2011).
[2] J.-Q. Yan, M. A. McGuire, A. F. May, H. Cao, A. D. Christianson, D. G. Mandrus, and B. C. Sales, Phys. Rev. B **87**, 104515 (2013).
[3] J.-Q. Yan, M. A. McGuire, A. F. May, D. Parker, D. G. Mandrus, and B. C. Sales, Phys. Rev. B **92**, 064507 (2015).
[4] F. Hulliger, Nature **209**, 500 (1966).
[5] Z. Bukowski, D. Badurski, J. Stepien-Damm, and R. Troc, Solid State Comm. **123**, 283 (2002).
[6] D. Parker, M. H. Du, and D. J. Singh, Phys. Rev. B **83**, 245111 (2011).
[7] C. Candolfi, B. Lenoir, C. Chubilleau, A. Dauscher, and E. Guilmeau, J. Phys.: Condens. Matter **22**, 025801 (2010).

[8] V. M. Dmitriev, L. F. Rybaltchenko, L. A. Ishchenko, E. V. Khristenko, Z. Bukowski, and R. Troc, Supercond. Sci. Technol. **19**, 573 (2006).
[9] V. M. Dmitriev, L. F. Rybaltchenko, E. V. Khristenko, L. A. Ishchenko, Z. Bukowski, and R. Troc, Low Temp. Phys. **33**, 295 (2007).
[10] C. Candolfi, B. Lenoir, A. Dauscher, J. Hejtmanek, E. Santava, and J. Tobola, Phys. Rev. B **77**, 092509 (2008).
[11] R. Khasanov, P. W. Klamut, A. Shengelaya, Z. Bukowski, I. M. Savic, C. Baines, and H. Keller, Phys. Rev. B **78**, 014502 (2008).
[12] V. H. Tran, W. Miller, and Z. Bukowski, Acta Mater. **56**, 5694 (2008).
[13] V. H. Tran, A. D. Hillier, D. T. Adroja, and Z. Bukowski, Phys. Rev. B **78**, 172505 (2008).
[14] R. Khasanov, A. Shengelaya, I. M. Savic, C. Baines, and H. Keller, Phys. Rev. B **82**, 016501 (2010).
[15] T. Koyama, H. Yamashita, Y. Takahashi, T. Kohara, I. Watanabe, Y. Tabata, and H. Nakamura, Phys. Rev. Lett. **101**, 126404 (2008).
[16] C. Candolfi, B. Lenoir, A. Dauscher, C. Bellouard, J. Hejtmanek, E. Santava, and J. Tobola, Phys. Rev. Lett. **99**, 037006 (2007).
[17] V. H. Tran, R. T. Khan, P. Wisniewski, and E. Bauer, J. Phys.: Conf. Ser. **273**, 012088 (2011).
[18] P. Jesnen and A. Kjekshus, Acta Chem. Scand. **20**, 417 (1966).
[19] V. H. Tran, W. Miiller, and Z. Bukowski, Phys. Rev. Lett. **100**, 137004 (2008).
[20] V. H. Tran, A. D. Hillier, D. T. Adroja, Z. Bukowski, and W. Miiller, J. Phys.: Condens. Matter **21**, 485701 (2009).
[21] T. Koyama, H. Yamashita, T. Kohara, Y. Tabata, and H. Nakamura, Mater. Res. Bull. **44**, 1132 (2009).
[22] H. Okabe, S. Yano, T. Muranaka, and J. Akimitsu, J. Phys.: Conf. Ser. **150**, 052196 (2009).
[23] N. Mori, H. Takahashi, and N. Takeshita, High Pressure Research **24**, 225 (2004).
[24] Y. Uwatoko, K. Matsubayashi, T. Matsumoto, N. Aso, M. Nishi, T. Fujiwara, M. Hedo, S. Tabata, K. Takagi, M. Tado, and H. Kagi, Rev. High Press. Sci. Tech. **18**, 230 (2008).
[25] J.-G. Cheng, K. Matsubayashi, S. Nagasaki, A. Hisada, T. Hirayama, M. Hedo, H. Kagi, and Y. Uwatoko, Rev. Sci. Instrum. **85**, 093907 (2014).
[26] P. Blaha, K. Schwarz, G. K. H. Madsen, D. Kvasnicka, and J. Luitz, *WIEN2k, An Augmented Plane Wave + Local Orbitals Program for Calculating Crystal Properties* (Techn. Universitat Wien, Austria, 2001).
[27] T. Moriya, in *Spin Fluctuations in Itinerant Electron Magnetism* (Springer, Berlin, 1985).
[28] T. Moriya and T. Takimoto, J. Phys. Soc. Jpn. **64**, 960 (1995).
[29] G. Bilbro and W. L. McMillan, Phys. Rev. B **14**, 1887 (1976).
[30] R. C. Lacoe, S. A. Wolf, P. M. Chaikin, C. Y. Huang, and H. L. Luo, Phys. Rev. Lett. **48**, 1212 (1982).
[31] G. F. Chen, K. Matsubayashi, S. Ban, K. Deguchi, and N. K. Sato, Phys. Rev. Lett. **97**, 017005 (2006).
[32] T. P. Orlando, E. J. J. McNiff, S. Foner, and M. R. Beasley, Phys. Rev. B **19**, 4545 (1979).
[33] A. Subedi, L. Zhang, D. J. Singh, and M. H. Du, Phys. Rev. B **78**, 134514 (2008).
[34] S. Nazir, S. Auluck, J. J. Pulikkotil, N. Singh, and U. Schwingenschlogl, Chem. Phys. Lett. **504**, 148 (2011).
[35] W. L. McMillan, Phys. Rev. **167**, 331 (1968).